

Do You See What I Am Pointing At?

Gesture-Based Egocentric Video Question Answering

Yura Choi¹, Roy Miles², Rolandos Alexandros Potamias¹

Ismail Elezi², Jiankang Deng¹, Stefanos Zafeiriou¹

¹Imperial College London ²Huawei Noah’s Ark Lab, UK

<https://yuuraa.github.io/papers/choi2026egovqa>

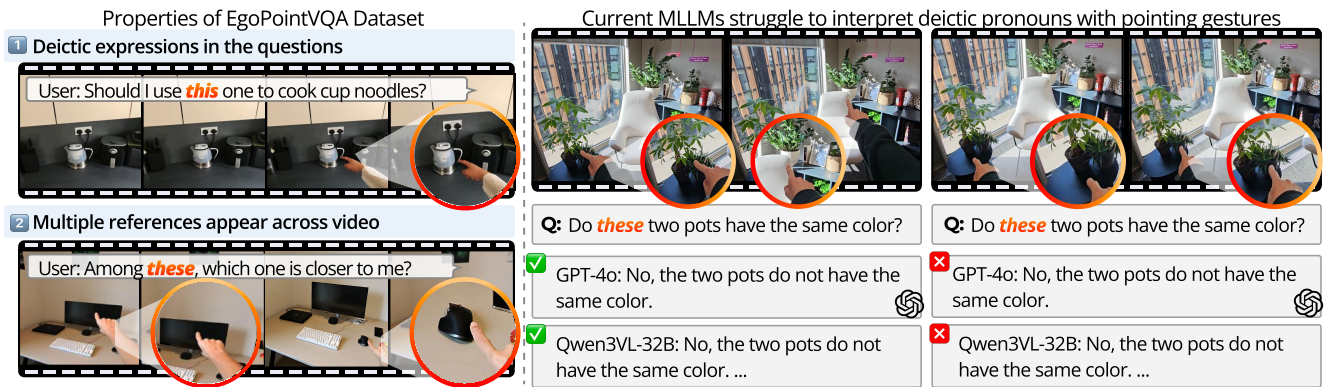


Figure 1. **Illustration of EGOPOINTVQA.** Left: EGOPOINTVQA includes questions with deictic pronouns requiring gesture understanding, either identifying single pointed objects (top) or tracking multiple references across frames (bottom). Right: State-of-the-art models, including GPT-4o [20] and Qwen3-VL-32B [37], fail to resolve the question with pointing gestures, incorrectly stating the two pots have different colors despite both being black. Zoomed circles highlight the pointed objects.

Abstract

Understanding and answering questions based on a user’s pointing gesture is essential for next-generation egocentric AI assistants. However, current Multimodal Large Language Models (MLLMs) struggle with such tasks due to the lack of gesture-rich data and their limited ability to infer fine-grained pointing intent from egocentric video. To address this, we introduce EGOPOINTVQA, a dataset and benchmark for gesture-grounded egocentric question answering, comprising 4000 synthetic and 400 real-world videos across multiple deictic reasoning tasks. Built upon it, we further propose Hand Intent Tokens (HINT), which encodes tokens derived from 3D hand keypoints using an off-the-shelf reconstruction model and interleaves them with the model input to provide explicit spatial and temporal context for interpreting pointing intent. We show that our model outperforms others in different backbones and model sizes. In particular, HINT-14B achieves 68.1% accuracy, on average over 6 tasks, surpassing the state-of-the-art, InternVL3-14B, by 6.6%. To further facilitate the open research, we will release the code, model, and dataset.

1. Introduction

As AI assistants become deeply integrated into daily wearable devices, from augmented and virtual reality (AR/VR) platforms like the Apple Vision Pro and Meta Orion to smart glasses like Meta Ray-Ban [29, 39] with built-in cameras, their ability to understand a user’s attention within their environment becomes essential [24, 32, 35, 45]. In particular, it is important to resolve spatial references through pointing gestures and deictic expressions (e.g., “Should I use *this* one?”), which are natural in human communication [8, 40, 43]. Thus, an AI assistant must understand not just what it sees, but also where the user is directing their attention. Typically, this requires: (1) identifying the deictic expression within the question that depends on gesture for meaning, (2) interpreting the hand’s movement and pose to understand the user’s referential intent, and (3) grounding this intent to identify the referred object and generate an appropriate response.

Despite the rapid progress of Multimodal Large Language Models (MLLMs), such gesture-aware and region-

specific question answering remains largely unexplored. From examples in Fig. 1, we observe that even state-of-the-art MLLMs fail to address questions grounded in the user’s gesture. This can be primarily attributed to two issues. First, the datasets these MLLMs are trained on contain limited gesture-rich video data, especially those capturing natural pointing behavior and egocentric interactions between users and nearby objects. As a result, models rarely encounter examples where gestures and deictic language co-occur in realistic contexts. Second, current architectures are not designed to explicitly encode or reason about gesture information. Most MLLMs integrate visual and textual inputs globally, without mechanisms to interpret hand positions or pointing directions. Consequently, they struggle to connect deictic expressions like “these” to the correct objects being referenced.

To address this, we introduce EGOPOINTVQA, a dataset composed of 4,000 synthetic and 400 real egocentric videos. These videos feature multiple objects and are specifically designed to support questions such as “What is the object I am pointing to?”, “How many objects of this type are there?”, or “What is the order of the objects I am pointing at?”. To enable systematic evaluation, we benchmark several models across our deictic task categories. Our evaluation benchmark contains 672 question–answer pairs over 300 real-world egocentric videos. Unlike prior egocentric video question answering (VQA) datasets that emphasize general scene understanding, EGOPOINTVQA focuses on fine-grained region-level reasoning, requiring both temporal and spatial comprehension to resolve gesture-based references accurately.

While training and benchmarking on this dataset helps mitigate the problem, the model must also explicitly attend to gestures. To achieve this, we introduce **Hand Intent Tokens (HINT)**, which are gesture-aware tokens, offering a compact representation and allowing the model to better interpret the user’s intent. We obtain 3D hand keypoints for each frame of the video using an off-the-shelf hand reconstruction model, and pass them through a lightweight adapter to produce frame-aligned hand-intent tokens.

We then insert these tokens into the MLLM input sequence alongside the corresponding visual tokens, so the model receives an explicit gesture stream in addition to video and text. This design allows the MLLM to associate hand motion and pointing direction with the question and answer, leading to more precise grounding of deictic expressions (e.g., “this one”). In the experimental section, we demonstrate that training with gesture tokens on deictic questions improves performance by 6.5% over standard fine-tuning, and surpasses the baseline by 8.6%.

In summary, our contributions are the following:

- We **introduce** EGOPOINTVQA, the first dataset specifically designed for deictic question answering in egocen-

tric videos, where user gestures and pointing behaviors are central to interpretation.

- We **propose** HINT, a simple yet effective approach that encodes gesture tokens derived from off-the-shelf 3D hand keypoints and interleaves them with the model input, providing explicit spatial and temporal context for interpreting pointing intent.
- We **demonstrate** that HINT achieves state-of-the-art performance on gesture-grounded question answering tasks, outperforming existing MLLMs and establishing a strong foundation for future research.

2. Related Work

Egocentric video question answering. The field of egocentric video question answering (VQA) has emerged as a critical challenge, established by foundational large-scale egocentric video datasets [6, 9, 17, 33]. Building upon these rich video corpora, dedicated VQA benchmarks were developed to specifically test complex reasoning about the wearer’s actions and environment [1, 7, 13, 22, 28, 31, 36, 52]. Benchmarks such as EgoThink [5] and VidEgoThink [4] focus on questions written in first-person perspective. Recently, EgoGPT [47] attempted to fine-tune MLLM [25] on wearer-perspective data, achieving improved performance on egocentric QA benchmarks [47]. Similarly, Ego-R1 [38] introduced a chain-of-tool-thought agent to reason over ultra-long first-person videos by decomposing queries and using external tools. These works mostly focus on long-term memory retrieval, habit analysis, or high-level queries. However, none address region-specific ambiguities: current MLLMs fail to resolve deictic questions (e.g., “what is this?”) when the referent is only indicated via a pointing gesture.

Region-specific visual question answering. Region-level question answering has progressed rapidly in the image domain, with MLLMs like Ferret [48], Osprey [49], and DAM [27] grounded language to arbitrary image regions. In video, methods like Artemis [14] track a specified region of interest across frames, while others like Elysium [41] and Omni-RGPT [18] use key frames or learnable tokens to represent the region features. Recently, large-scale datasets like VideoInfer [50] have been built to train this capability. However, all these works assume a referred region is explicitly given in the form of bounding box coordinates, segmentation masks, or a scribble. In contrast, our work tackles the more natural scenario where the region of interest must be inferred implicitly from a human’s pointing gesture captured within the egocentric video itself.

Visual prompting for MLLMs. Providing additional visual cues or prompts has proven effective for steering MLLMs towards fine-grained understanding [44]. These can be artificial overlays like alphanumeric tags [46], user-drawn scribbles [2, 42], or 2D points [10]. These meth-

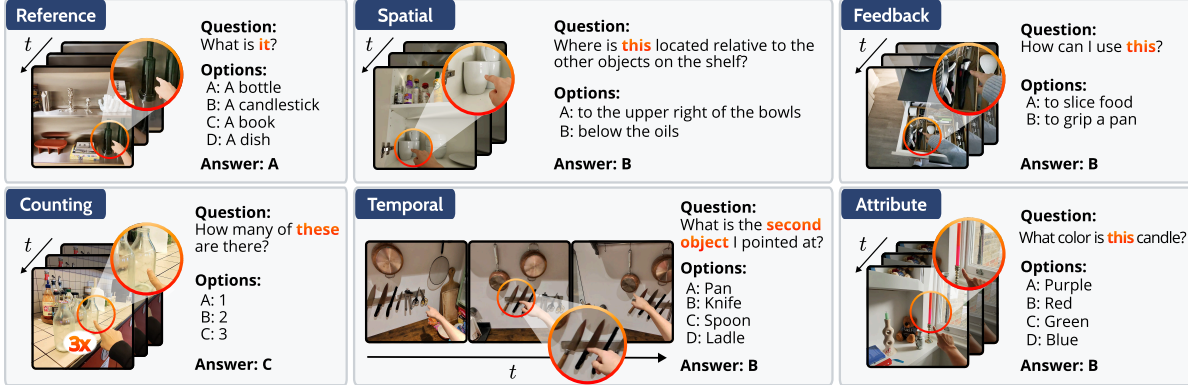


Figure 2. **Task taxonomy and examples from EGOPOINTVQA.** EGOPOINTVQA includes six subsets of questions regarding the properties of a pointed object. Each example shows egocentric video frames and a question using deictic references. Tasks include reference (object identification), counting (number of same objects), spatial (location and relative depth), temporal (order of multiple gestures), attribute (object properties), and feedback (object function). All questions require resolving deictic references through visual grounding of pointing gestures. The pointed objects are highlighted with red circles for visualization purposes.

ods prove that MLLMs can learn to interpret visual cues, but they all rely on artificial, non-natural prompts. Our work departs from this paradigm by treating a natural human cue, already present in the egocentric video, through explicit hand tokens. While other research has leveraged other natural signals like gaze to interpret the wearer’s focus and align language with visual intent [32, 45], our work tackles the distinct and complementary challenge of interpreting the pointing gesture. Our approach of converting 3D hand keypoints into continuous hand tokens and interleaving them with the model’s input sequence is a novel method for explicitly conditioning an MLLM on natural, pointing gestures for VQA.

3. EGOPOINTVQA Dataset

We introduce EGOPOINTVQA, the first dataset for pointing gesture-based question answering in egocentric video. The dataset combines both real-world and synthetic videos, each paired with multiple-choice question-answer pairs asking about specific regions and objects visible in the video. We describe the task in §3.1, the video collection in §3.2, and the question and answer generation in §3.3.

3.1. Task Definition

Given an egocentric video containing one or more pointing gestures, where each gesture is associated with a target object at a specific timestamp, our task is to answer natural language deictic questions about the pointed objects. A deictic question is formulated in first-person perspective and contains pronouns where the referent cannot be determined without visual and gestural context. Common deictic expressions include demonstratives (e.g., “this”, “that”, “those”), spatial indications (“here”, “there”), and temporal references (“the second object I pointed at”). Unlike standard video QA, where questions unambiguously describe

the target object, deictic questions intentionally omit explicit descriptions, requiring the model to infer the referent from the user’s pointing gesture. To answer these questions, the system must jointly perform: (1) the spatial-temporal alignment between hand pose and objects to resolve what is being pointed at, (2) the linguistic grounding of deictic expressions to the visual scene, and (3) object properties, relations, and scene context to produce the correct answer.

Task taxonomy. As illustrated in Fig. 2, we decompose deictic question answering into six question categories, each testing distinct reasoning capabilities.

- *Reference* – e.g., when asked “What is it?” while the user is pointing to an item on a shelf, the model must correctly identify this object.
- *Counting* – determining the number of identical or similar objects in a view.
- *Spatial* – understanding the relative position of the referenced object with respect to other objects in the scene.
- *Temporal* – interpreting references when multiple pointing gestures occur in a sequence, using their order to resolve ambiguity.
- *Feedback* – answering context-aware queries about an object’s function or relevance to the user’s goal.
- *Attribute* – identifying properties such as color, shape, or material of the referenced object.

3.2. Video Collection

To construct a comprehensive dataset, we draw from both synthetic and real-world egocentric videos. Synthetic data allows us to overcome large-scale annotation challenges by providing precise control over object placement, viewpoint, and gesture timing. In contrast, real videos capture the natural variability and complexity of human behavior. Accordingly, our training set is predominantly synthetic with a small subset of real videos, while our test set comprises

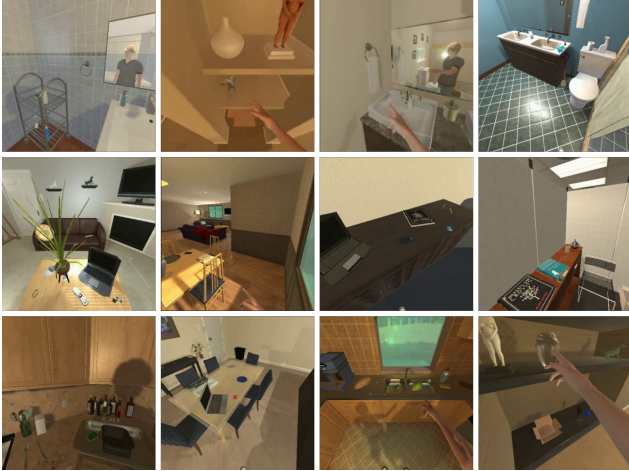


Figure 3. **Visualization of synthetic videos in EGOPOINTVQA.** Our synthetic data covers diverse indoor scenes with various lighting conditions.

exclusively of real-world footage.

Synthetic video generation pipeline. We generate 4,000 synthetic videos using AI2-THOR [23], a photorealistic 3D simulator with 184 diverse indoor scenes. From these scenes, we sample 12,000 viewpoints containing at least three visible nearby small objects, and select a subset of visible objects as target objects for pointing questions. We create the pointing gestures by adapting MIXAMO animations [21] using inverse kinematics to ensure the index finger aligns with the selected object. We then render the videos as 3–5 second clips at 30 frames per second (FPS) with 448×448 resolution. Finally, we apply automatic quality filtering, retaining only those clips where the referenced object remains visible in at least 50% of frames and the hand is reliably visible in over 60% of the frames. As visualized in Fig. 3, generated videos show objects at diverse locations, with varied lighting.

Real video collection. To construct a realistic evaluation scenario, we collect 400 egocentric videos using Meta Ray-Ban smart glasses [39]. We recruit 20 participants and instruct them to naturally point at objects in their daily environment, where more than 3 objects are visible. These recordings took place across indoor (living room, kitchen, offices) and outdoor (streets, parks) settings (360 indoor and 40 outdoor). Each clip ranges from 3–8 seconds with 30FPS, on average, at 1536×2048 resolution. We allocate 100 videos for training (combined with synthetic data) and reserve 300 videos exclusively for evaluation.

3.3. Question and Answer Generation

We design an automated pipeline to generate multiple-choice question-answer pairs from synthetic and real egocentric videos. Generating descriptive questions about target objects requires two key capabilities: precise object localization across temporal sequences and a rich semantic

understanding of spatial, temporal, and visual attributes. To achieve this, our pipeline operates in three stages as illustrated in Fig. 4: we first extract dense descriptions and metadata for the video, then we generate structured questions that reference the target objects, and finally, we transform the questions into natural first-person deictic expressions. For real videos used in the evaluation, we perform manual verification and refinement to ensure high quality.

Stage 1: Extracting dense scene information. The goal of this stage is to extract comprehensive scene information to automatically generate high-quality question-answer pairs. The process differs between synthetic and real videos. For synthetic videos, we leverage the simulator’s API to extract depth maps, object-wise segmentation masks, categories, and 3D location. Since the simulator does not provide all visual attributes (e.g., color), we supplement this by running an annotator MLLM (InternVL3-78B [53]) per object to extract these properties. For real videos, we first generate scene metadata for all visible objects. We follow a pipeline of SpatialRGPT [3] to obtain dense object-wise scene descriptions with segmentation masks. To establish a precise ground-truth for our pointing task, we manually annotate the bounding box of the specific target object (i.e., the object being pointed at). We store this information as a list of JSON dictionaries, with each dictionary detailing a single object.

Stage 2: Target-specific multiple-choice question answer generation. Using the comprehensive scene information from Stage 1, we generate multiple-choice question-answer pairs. We first generate template-based question answer pairs that are specific to each of our six task categories. Given example questions, videos, and the rule-based question-answer pairs, the annotator MLLM generates question-answer pairs that refer to the pointing target object using the object id placeholder. For example, an ‘Attribute’ question is generated using a template like ‘What color is <object2>?’. We populate the negative answers based on the visible objects’ metadata. After constructing the structured question-answer pairs, we prompt the question-generating MLLM to produce a set of plausible hard negative options based on the scene information, visual input, and textually coherent alternatives.

Stage 3: Question rephrasing. We convert the questions from Stage 2 into natural queries. We feed the multiple-choice QA pairs into GPT-4o [20], which rephrases them by replacing object identifiers (e.g., <object2>) with contextually appropriate deictic pronouns (e.g., “this”, “it”).

Quality control. We manually inspect every proposed question-answer pair for our 300 real-world evaluation videos. We have two criteria: (1) correctness: the question and answer correspond with the video, (2) deictic ambiguity: the question is formulated using indirect pronouns. This ensures the question is difficult or impossible to answer cor-

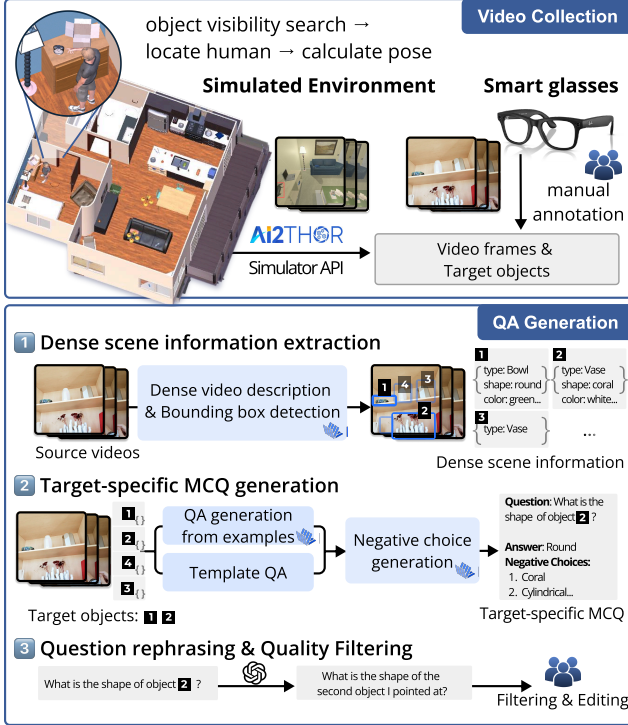


Figure 4. **EGOPOINTVQA generation pipeline.** From a mixture of simulated and real egocentric videos, we automatically generate multiple-choice question answer pairs referring to the pointed objects in the video. The questions are made deictic so that the model should visually understand the pointing gesture to answer.

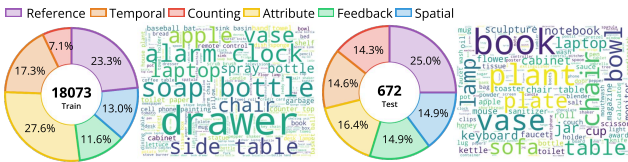


Figure 5. **EGOPOINTVQA statistics.** Distribution of task types (charts) and common object word clouds for the (Left) training set (N=18073) and the (Right) test set (N=672).

rectly without understanding the pointing gesture.

Dataset statistics. In Fig. 5, we visualize statistics and common object word clouds of EGOPOINTVQA. The dataset contains 4,000 synthetic videos and 400 real videos with a total of 18,745 question-answer pairs. It is split into two subsets: an instruction tuning (training) set that contains whole synthetic videos and their QA pairs, supplemented with 100 real videos and their 640 QA pairs, and the test set of 300 real videos with 672 QA pairs.

4. Hand Intent Tokens

Given an egocentric video, represented as a sequence of frames $\{I_1, I_2, \dots, I_T\}$ and a deictic question in text, our goal is to generate the correct answer. Current MLLMs struggle with such deictic queries because they often fail

to (1) recognize that the question alone is ambiguous, and (2) accurately identify the user’s referential intent behind the pointing gesture. To address these challenges, we introduce HINT, a model that processes the video in two parallel streams: a standard visual stream (§4.1) and a new hand-intent stream (§4.2). As shown in Fig. 6, we develop a lightweight *Keypoint Adapter* that converts 3D hand pose features from an off-the-shelf hand reconstruction model into a sequence of *hand intent tokens*. We then interleave these gesture tokens with the visual tokens (§4.3) and feed the combined sequence into the MLLM, providing explicit pointing information that helps resolve deictic ambiguity.

4.1. Visual Token Extraction

The primary visual stream follows the standard MLLM architecture. Each video frame I_t is passed through a Vision Encoder (e.g., InternViT [53]) followed by a Vision Projector (an MLP). This process maps the raw image into a sequence of embedding vectors (i.e., visual tokens), which we denote as V_t , and represents the visual content of the frame in the backbone LLM’s embedding space.

4.2. Hand Intent Token Extraction

3D hand pose extraction. Interpreting a referential gesture requires accurate estimation of the hand’s 3D pose. This pose is the primary signal of referential intent, distinguishing a deliberate pointing action from other incremental hand motions. Consequently, our pipeline includes a 3D hand reconstruction module for estimating the hand pose in each frame. We choose to use WiLoR [34] for this task since it has demonstrated robustness on in-the-wild images. For each frame I_t , WiLoR outputs 3D camera space coordinates of 21 hand keypoints K_t . These keypoints provide a geometric representation of the hand’s configuration per frame, which serves as the input to our Keypoint Adapter.

Keypoint adapter. The role of this adapter is to project the 21 distinct 3D keypoints $K_t \in \mathbb{R}^{21 \times 3}$ into a single Hand Intent Token H_t that holistically represents the entire posture of the hand for that frame:

$$\tilde{k}_t = \text{flatten}(K_t) \in \mathbb{R}^{63}, \quad (1)$$

$$H_t = \begin{cases} W_2 \sigma(W_1 \text{LN}(\tilde{k}_t)), & \text{if } c_t \geq \tau \\ \emptyset, & \text{otherwise,} \end{cases} \quad (2)$$

where $W_1 \in \mathbb{R}^{d_h \times 63}$, $W_2 \in \mathbb{R}^{d \times d_h}$, σ is GeLU, c_t is the confidence of the hand detection, LN is LayerNorm, d_h the hidden size, and d matches the width of the LLM. Here, \emptyset denotes the absence of a hand-intent token when $c_t < \tau$, i.e., no gesture token is inserted at time t . This cheap adapter keeps latency low while exposing the LLM to compact frame-aligned gesture tokens.

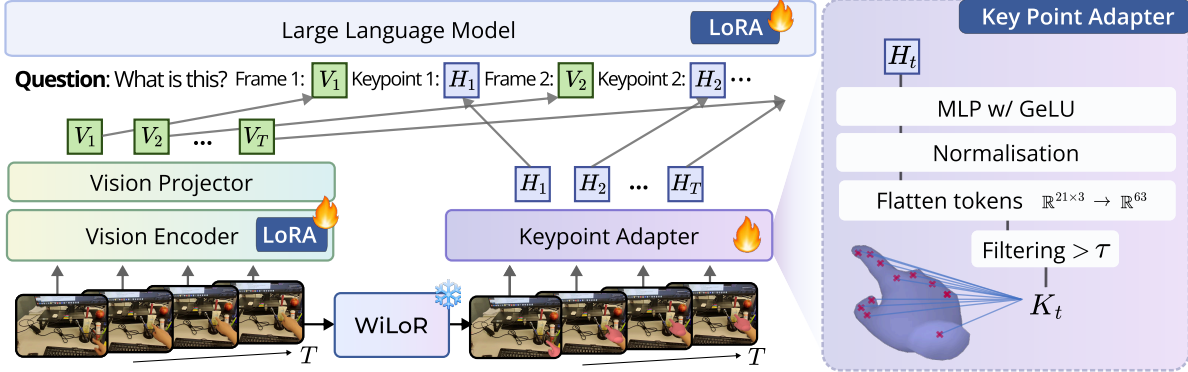


Figure 6. **HINT overall architecture.** HINT uses an additional adapter to model the 3D location and movement of the hand directly. V_t denotes a visual token, K_t the keypoint feature, and H_t the hand intent token extracted for each frame I_t .

4.3. Frame-Keypoint Interleaving.

We interleave hand intent tokens with visual tokens so the LLM can jointly reason over *what* has happened and *where the user has pointed*. An example of a question and its answer in the dataset is as follows:

Question: What is this? A. a toothpaste B. a monitor ...

Frame-1: $\langle vis \rangle$ Keypoint-1: $\langle key \rangle$... Answer: A.

For each $\langle vis \rangle$ token, we use the corresponding vision tokens V_t ; likewise, for each $\langle key \rangle$ token, we use the corresponding keypoint tokens H_t produced by the keypoint adapter. To cover the case where there is no hand present in the frame, we only interleave keypoint tokens if the detection confidence (given by WiLoR) exceeds $\tau = 0.5$. This allows the model to naturally handle videos with intermittent hand visibility, a common occurrence in egocentric videos where hands move in and out of frame.

Since the HINT tokens are interleaved with the input sequence, the LLM will be temporally conditioned on them. For a sequence of length L , the probability of generating the target answers \mathbf{X}_a is given by:

$$p(\mathbf{X}_a | \mathbf{V}, \mathbf{X}_q, \mathbf{H}) = \prod_{i=1}^L p(x_i | \mathbf{V}, \mathbf{X}_{q, < i}, \mathbf{X}_{a, < i}, \mathbf{H}_{< i}), \quad (3)$$

where $\mathbf{X}_{q, < i}$, $\mathbf{X}_{a, < i}$, and $\mathbf{H}_{< i}$ denote the instruction, answer and HINT tokens preceding the current prediction token. For the conditionals in (3), we explicitly add \mathbf{H} to highlight that all answer tokens are grounded in the hand signal. This interleaved construction enables the LLM to jointly understand deictic context and the user’s temporally anchored references.

5. Experiments

We conduct a series of experiments to establish the challenge of our EGOPOINTVQA benchmark by evaluating several state-of-the-art MLLMs, and perform an analysis of our proposed HINT method, ablating its core components.

5.1. Experimental Setup

Evaluation benchmark and metrics. We conduct all experiments on the EGOPOINTVQA test set, which consists of 300 real-world indoor and outdoor videos. We report the multiple-choice accuracy (Acc. %) for each of the six task categories along with the overall average accuracy. For a fair comparison, all video MLLMs process 32 uniformly sampled frames per video.

Baseline models. We evaluate 15 models spanning three categories: (1) proprietary models including GPT-5 [30], and GPT-4o [20]; (2) Open-source generalist MLLMs, including Qwen3-VL [37] (8B, 32B), LLaVA-OneVision [25] (7B, 72B), InternVL2.5 [12] (8B, 38B), and InternVL3 [53] (8B, 14B, 38B, 78B); and (3) models with relevant specializations including EgoGPT-7B [47] (egocentric video understanding), VGLLM-QA-8B [51] (3D geometry understanding), and Vispeak [16] (visual instruction).

HINT implementation. We implement HINT on three representative backbones: LLaVA-OneVision-7B, InternVL3-8B, and InternVL3-14B. We use WiLoR [34] to extract 3D hand keypoints, setting 0.5 as the detection confidence threshold τ . We train the Keypoint Adapter from scratch, and fine-tune using LoRA [19] the vision encoder and LLM. We optimize hyperparameters such as LoRA rank, alpha, and learning rate for each backbone individually. We optimize all models using AdamW with a cosine schedule and a batch size of 32 for one epoch on our mixed synthetic-real training dataset. We provide a detailed list of the hyperparameters in the Appendix.

5.2. Main Results

Zero-shot existing model performance. The results in Table 1 show that EGOPOINTVQA poses a challenge for any model. All models achieve an average accuracy below 70%. Among baseline models under 10B parameters, EgoGPT-7B achieves the highest reference accuracy at 67.3%. Particularly, comparing the Reference task with the Temporal tasks, even top models like GPT-5 show a dramatic drop.

Method	Size	LLM	Refer.	Temporal	Spatial	Count	Attr.	Feed.	Avg.
Random	-	-	20.0	20.0	27.0	20.0	20.0	50.0	26.2
<i>Proprietary Models</i>									
GPT-5 [30]	-	-	75.6	53.6	62.3	50.0	56.1	77.8	62.6
GPT-4o [20]	-	-	56.1	29.5	43.1	44.8	41.5	65.7	46.8
<i>Open-source MLLMs $\geq 32B$</i>									
Qwen3-VL [37]	32B	Qwen3	63.7	67.9	65.8	66.7	63.4	77.2	67.5
InternVL2.5 [12]	38B	InternLM2.5	61.3	57.1	60.5	39.6	63.4	77.2	59.9
InternVL3 [53]	38B	InternLM3	70.2	67.9	65.8	45.8	65.9	78.9	65.8
LLaVA-OneVision [25]	72B	Qwen2	61.3	44.6	60.5	41.7	51.2	72.3	55.3
InternVL3 [53]	78B	InternLM3	71.4	71.4	62.3	45.8	68.3	80.1	66.6
<i>Open-source MLLMs $\leq 8B$</i>									
InternVL2.5 [12]	8B	InternLM2.5	54.2	41.1	59.6	37.5	63.4	77.2	55.5
Qwen3-VL [37]	8B	Qwen3	61.9	53.6	56.1	35.4	48.8	79.4	55.9
ViSpeak [16]	7B	Qwen2	65.5	42.9	48.2	39.6	51.2	70.2	52.9
EgoGPT [47]	7B	Qwen2	67.3	46.4	50.9	47.9	48.8	74.1	55.9
VGLLM-QA [51]	8B	Qwen2.5	57.7	35.7	53.5	39.6	36.6	70.2	48.9
LLaVA-OneVision [25]	7B	Qwen2	54.2	42.9	53.5	35.4	46.3	67.1	49.9
HINT _{LLaVA-OneVision}	7B	Qwen2	60.7	50.0	56.1	39.6	48.8	71.1	54.4
InternVL3 [53]	8B	InternLM3	66.1	57.5	63.2	33.3	51.3	76.8	58.0
HINT _{InternVL3-8B}	8B	InternLM3	75.0	66.1	64.9	35.4	61.0	79.8	63.7
InternVL3 [53]	14B	InternLM3	63.1	66.1	61.4	50.0	58.5	77.2	62.7
HINT _{InternVL3-14B}	14B	InternLM3	73.8	69.6	64.9	54.2	63.4	82.5	68.1

Table 1. **Performance of different MLLMs on EGOPOINTVQA test set.** We report multiple-choice accuracy (%). HINT (light blue rows) consistently and significantly improves performance over its corresponding open-source backbones, outperforming all baseline models. Task categories are: Reference (Refer.), Temporal, Spatial, Counting (Count), Attribute (Attr.), and Feedback (Feed.). In the bottom rows, we report the performance of HINT applied to three baselines, highlighted in light blue.

This shows that tracking multiple gestures across time requires fundamentally different capabilities than single gesture understanding. We also observe that specialization provides limited benefits. Despite strong performance on related benchmarks, models with relevant knowledge show small advantages in gesture understanding, e.g., EgoGPT reaches the best Reference and Counting accuracy among small models, but fails on temporal sequences.

Impact of model scaling. Scaling within model families generally offers modest gain in performance. For instance, the Reference accuracy of Qwen3-VL improves from 61.9% (8B) to 63.7% (32B), and InternVL3 improves from 66.1% (8B) to 70.2% (38B) to 71.4% (78B). This pattern suggests that while enhanced reasoning capability with a larger LLM backbone helps, the major bottleneck lies in the absence of explicit gesture understanding.

Performance improvement with HINT. As shown in Table 1, HINT demonstrates consistent improvements across all backbones and task categories. The method’s primary impact is on the core grounding challenge, which is most evident in the Reference task. Here, we see the largest gains, such as +10.7 percentage points (*pp*) for InternVL3-14B (63.1% \rightarrow 73.8%) and +8.9 *pp* for InternVL3-8B (66.1%

SFT	Hand Int.	Reference	Temporal	Spatial	Attribute
✗	✗	66.1	57.5	63.2	51.3
✓	✗	68.5	60.7	59.6	56.7
✓	✓	75.0	66.1	64.9	61.0

Table 2. **Ablation of HINT components.** ‘SFT’ denotes supervised fine-tuning on EGOPOINTVQA. ‘Hand Int.’ denotes use of our Hand Intent Token. Combining both yields the largest gains.

\rightarrow 75.0%). This improved grounding also leads to gains in other tasks, though the effect varies by backbone. For instance, the InternVL3-8B also sees large boosts in the Temporal (+8.6*pp*) and Attribute (+9.7*pp*) tasks. Similarly, HINT improves LLaVA-OneVision, reaching an average improvement of 4.5*pp* across the six tasks.

Computational cost and token overhead. We measure inference time on 32-frame inputs using the InternVL3-8B backbone. Without hand keypoint extraction and the keypoint adapter, the inference takes 2.58s, while using the HINT tokens increases the time only to 2.84s. Moreover, with a threshold of $\tau = 0.5$, the HINT tokens account for less than 1% of the total tokens fed to the LLM.

Real	Synthetic	Reference	Temporal	Spatial	Attribute
✗	✓	69.0	62.5	60.5	58.5
✓	✗	67.3	60.7	56.1	56.1
✓	✓	75.0	66.1	64.9	61.0

Table 3. **Impact of training dataset.** We vary the usage of synthetic and real videos in the training set. Using a synthetic dataset to complement a real dataset yields the best result.

Hand Intent Modeling	Reference	Temporal	Spatial
None	68.5	60.7	59.6
Visual Keypoints	57.1	60.7	61.4
Visual Arrow from Fingertip	70.2	60.7	62.3
3D Keypoints in Text	68.5	55.4	58.8
2D Keypoints in Text	69.0	57.1	59.6
HINT	75.0	66.1	64.9

Table 4. **Different methods of hand intent modeling.** We compare different methods to encode the user’s hand pose. Our HINT with learning keypoint adapter outperforms alternative representations, such as visual prompts and textual inputs.

5.3. Ablation Study and Analysis

For consistency, unless specified otherwise, we perform all ablations using InternVL3-8B.

Ablation of proposed components. In Table 2, we analyze the contribution of each component of our method. Supervised fine-tuning (SFT) on the EGOPOINTVQA training data alone offers a small benefit, improving Reference accuracy from 66.1% to 68.5%. However, combining SFT with HINT achieves 75.0% on the same task. This demonstrates that simply exposing the model to gesture-based questions is insufficient, thus the explicit architectural component to process the 3D hand pose signal is necessary.

Impact of training data composition. In Table 3, we show how adding synthetic data to the real training set affects the performance. Training on real videos only achieves 67.3% on reference and 60.7% on temporal tasks. Mixing the two datasets yields the best results.

Hand intent modeling methods. We test multiple methods to feed gesture information to the model, reported in Tab. 4. We test naive visual prompting strategies with two variations, where we plot the information of the user’s hand onto the video frame, both of which show be ineffective. Plotting visual keypoints on the frames harms the performance on the reference task, while drawing visual arrows from the fingertip provides a moderate boost but is still sub-optimal (70.2%). Input keypoint coordinates along with the video perform moderately (68.5-69.0% in the reference task). Our learned keypoint encoder outperforms all alternatives (75.0% reference), suggesting that allowing the model to learn how to process geometric hand information is more effective than providing it through visual or textual formats.

Impact of hand detection confidence threshold τ . In Tab. 5, we analyze the impact of the hand detection confi-

τ	Reference	Temporal	Spatial	Count	Attribute
0.1	66.7	58.7	62.9	32.4	59.3
0.3	75.0	58.7	62.9	35.3	59.3
0.5	75.0	66.1	64.9	35.4	61.0
0.7	64.9	60.9	62.9	32.4	59.3
0.9	68.4	63.1	60.0	32.4	59.3

Table 5. **Impact of hand detection confidence threshold τ on HINT.** The threshold τ controls a trade-off between filtering noisy detections and retaining valid pointing gestures. A value of 0.5 achieves the best overall performance.

Method	Input Frames	Reference	Spatial	Attribute
InternVL3-8B	uniform 32	66.1	63.2	51.3
InternVL3-8B	keyframes	61.3	62.3	61.0
InternVL3-14B	uniform 32	63.1	61.4	58.5
InternVL3-14B	keyframes	60.1	56.1	61.2

Table 6. **Inference with keyframes.** We feed the model only the ‘keyframes’ when the pointing gesture is most clearly seen. Per pointing gesture, we select one frame to feed into the model.

dence threshold τ , which controls a trade-off between retaining valid gesture signals and filtering noise. A low threshold ($\tau \leq 0.3$) is too permissive, and the resulting noise harms performance on complex tasks like Temporal (58.7%) and Attribute (59.3%). Conversely, a high threshold ($\tau \geq 0.7$) is too strict, discarding valid gestures and causing Reference performance to drop (e.g., 64.9% at $\tau=0.7$). We find $\tau=0.5$ achieves the best overall balance, yielding the top results across all categories.

Impact of input frames. In Tab. 6, we compare the model performance when using uniformly sampled frames versus keyframes. For the keyframe condition, we feed the model the frames where the pointing gesture is most clearly visible (one keyframe per pointing gesture). This setting tests whether a keyframe is sufficient to resolve deictic references. The results demonstrate that, in practice, understanding pointing gestures requires temporal context beyond isolated keyframes, especially for the Reference task, where the model must directly identify the pointed object.

6. Conclusion

We introduced EGOPOINTVQA, the first dataset tailored for gesture-grounded egocentric video question answering, featuring 4,000 synthetic and 400 real-world videos. The accompanying benchmark enables rigorous evaluation of fine-grained spatial and temporal reasoning from pointing gestures. To advance gesture understanding, we proposed Hand Intent Tokens (HINT), a model that encodes 3D hand keypoints as tokens interleaved with visual and textual inputs, allowing effective interpretation of referential intent. Our method achieves state-of-the-art performance, outperforming open-source baselines by an average of 6.6%.

Acknowledgement

S. Zafeiriou and R. Potamias was funded by the EPSRC Project GNOMON (EP/X011364/1) and Turing AI Fellowship (EP/Z534699/1). J. Deng was supported by the NVIDIA Academic Grant.

References

- [1] Leonard Bärmann and Alex Waibel. Where did i leave my keys? - episodic-memory-based question answering on egocentric videos. In *CVPRW*, 2022. 2
- [2] Mu Cai, Haotian Liu, Dennis Park, Siva Karthik Mustikovela, Gregory P. Meyer, Yuning Chai, and Yong Jae Lee. Vip-llava: Making large multimodal models understand arbitrary visual prompts. In *CVPR*, 2024. 2
- [3] An-Chieh Cheng, Hongxu Yin, Yang Fu, Qiushan Guo, Ruihan Yang, Jan Kautz, Xiaolong Wang, and Sifei Liu. Spatial-rgpt: Grounded spatial reasoning in vision language models. In *NeurIPS*, 2024. 4
- [4] Sijie Cheng, Kechen Fang, Yangyang Yu, Sicheng Zhou, Bohao Li, Ye Tian, Tingguang Li, Lei Han, and Yang Liu. Videogothink: Assessing egocentric video understanding capabilities for embodied ai. *arXiv preprint*, 2024. 2
- [5] Sijie Cheng, Zhicheng Guo, Jingwen Wu, Kechen Fang, Peng Li, Huaping Liu, and Yang Liu. Egothink: Evaluating first-person perspective thinking capability of vision-language models. In *CVPR*, 2024. 2
- [6] Dima Damen, Hazel Doughty, Giovanni Maria Farinella, Sanja Fidler, Antonino Furnari, Evangelos Kazakos, Davide Moltisanti, Jonathan Munro, Toby Perrett, Will Price, and Michael Wray. The epic-kitchens dataset: Collection, challenges and baselines. *TPAMI*, 2020. 2
- [7] Shangzhe Di and Weidi Xie. Grounded question-answering in long egocentric videos. In *CVPR*, 2024. 2
- [8] Holger Diessel and Kenny R Coventry. Demonstratives in spatial language and social interaction: An interdisciplinary review. *Frontiers in Psychology*, 2020. 1
- [9] Kristen Grauman et al. Ego4d: Around the world in 3,000 hours of egocentric video. In *CVPR*, 2022. 2
- [10] Soroush Nasiriany et al. Pivot: Iterative visual prompting elicits actionable knowledge for vlms. *arXiv preprint*, 2024. 2
- [11] Xiao et al. Egoblind: Towards egocentric visual assistance for the blind. In *NeurIPS Datasets and Benchmarks Track*, 2025. 1
- [12] Zhe Chen et al. Expanding performance boundaries of open-source multimodal models with model, data, and test-time scaling. *arXiv preprint*, 2025. 6, 7
- [13] Chenyou Fan. EgoVQA-an egocentric video question answering benchmark dataset. In *CVPR*, 2019. 2
- [14] Renju Feng, Ning Xi, Duanfeng Chu, Rukang Wang, Zejian Deng, Anzheng Wang, Liping Lu, Jinxiang Wang, and Yanjun Huang. Artemis: Autoregressive end-to-end trajectory planning with mixture of experts for autonomous driving. In *NeurIPS*, 2025. 2
- [15] Chaoyou Fu, Yuhan Dai, Yongdong Luo, Lei Li, Shuhuai Ren, Renrui Zhang, Zihan Wang, Chenyu Zhou, Yunhang Shen, Mengdan Zhang, et al. Video-mme: The first-ever comprehensive evaluation benchmark of multi-modal llms in video analysis. In *CVPR*, 2025. 1
- [16] Shenghao Fu, Qize Yang, Yuan-Ming Li, Yi-Xing Peng, Kun-Yu Lin, Xihan Wei, Jian-Fang Hu, Xiaohua Xie, and Wei-Shi Zheng. Vispeak: Visual instruction feedback in streaming videos. In *ICCV*, 2025. 6, 7
- [17] Kristen Grauman et al. Ego-exo4d: Understanding skilled human activity from first-and third-person perspectives. In *CVPR*, 2024. 2
- [18] Miran Heo, Min-Hung Chen, De-An Huang, Sifei Liu, Subhashree Radhakrishnan, Seon Joo Kim, Yu-Chiang Frank Wang, and Ryo Hachiuma. Omni-rgpt: Unifying image and video region-level understanding via token marks. In *CVPR*, 2025. 2
- [19] Edward J. Hu, Yelong Shen, Phillip Wallis, Zeyuan Allen-Zhu, Yuanzhi Li, Shean Wang, Lu Wang, and Weizhu Chen. Lora: Low-rank adaptation of large language models. In *ICLR*, 2021. 6
- [20] Aaron et al. Hurst. Gpt-4o system card. *arXiv preprint*, 2024. 1, 4, 6, 7
- [21] Adobe Inc. Mixamo: 3d characters, skeletal rigs, and animations, 2021. 4, 3
- [22] Ting Jia, Baoxiong .and Lei, Song-Chun Zhu, and Siyuan Huang. Egotaskqa: Understanding human tasks in egocentric videos. *NeurIPS*, 2022. 2
- [23] Eric Kolve, Roozbeh Mottaghi, Winson Han, Eli VanderBilt, Luca Weihs, Alvaro Herrasti, Daniel Gordon, Yuke Zhu, Abhinav Gupta, and Ali Farhadi. AI2-THOR: An Interactive 3D Environment for Visual AI. *arXiv preprint*, 2017. 4, 3
- [24] Jaewook Lee, Jun Wang, Elizabeth Brown, Liam Chu, Sebastian S. Rodriguez, and Jon E. Froehlich. Gazepointer: A context-aware multimodal voice assistant for pronoun disambiguation in wearable augmented reality. *arXiv preprint*, 2024. 1
- [25] Bo et al. Li. Llava-onevision: Easy visual task transfer. *TMLR*, 2025. 2, 6, 7
- [26] Kunchang Li, Yali Wang, Yinan He, Yizhuo Li, Yi Wang, Yi Liu, Zun Wang, Jilan Xu, Guo Chen, Ping Luo, Limin Wang, and Yu Qiao. Mvbench: A comprehensive multimodal video understanding benchmark. In *CVPR*, 2024. 1
- [27] Long Lian et al. Describe anything: Detailed localized image and video captioning. In *ICCV*, 2025. 2
- [28] Karttikeya Mangalam, Raiymbek Akshulakov, and Jitendra Malik. Egoschema: A diagnostic benchmark for very long-form video language understanding. In *NeurIPS*, 2023. 2, 1
- [29] Meta Platforms, Inc. Meta ray-ban display: Ai-powered smart glasses. <https://www.meta.com/ai-glasses/meta-ray-ban-display/>, 2025. Accessed: 2025-09-19. 1
- [30] OpenAI. GPT-5 System Card, 2025. Accessed on March 16, 2026. 6, 7
- [31] Alkesh Patel, Vibhav Chitalia, and Yinfei Yang. Advancing egocentric video question answering with multimodal large language models. *arXiv: 2504.04550*, 2025. 2

- [32] Taiying Peng, Jiacheng Hua, Miao Liu, and Feng Lu. In the eye of MLLM: Benchmarking egocentric video intent understanding with gaze-guided prompting. In *NeurIPS*, 2025. 1, 3
- [33] Toby Perrett, Ahmad Darkhalil, Saptarshi Sinha, Omar Emara, Sam Pollard, Kranti Kumar Parida, Kaiting Liu, Prajwal Gatti, Siddhant Bansal, Kevin Flanagan, et al. Hd-epic: A highly-detailed egocentric video dataset. In *Proceedings of the Computer Vision and Pattern Recognition Conference*, pages 23901–23913, 2025. 2
- [34] Rolandos Alexandros Potamias, Jinglei Zhang, Jiankang Deng, and Stefanos Zafeiriou. Wilor: End-to-end 3d hand localization and reconstruction in-the-wild. In *CVPR*, 2025. 5, 6
- [35] Jun Rekimoto. Gazellm: Multimodal llms incorporating human visual attention. In *Proceedings of the Augmented Humans International Conference 2025*, 2025. 1
- [36] Ivan Rodin, Tz-Ying Wu, Kyle Min, Sharath Nittur Sridhar, Antonino Furnari, Subarna Tripathi, and Giovanni Maria Farinella. Easg-bench: Video q&a benchmark with egocentric action scene graphs. 2025. 2
- [37] Qwen Team. Qwen3 technical report, 2025. 1, 6, 7
- [38] Shulin Tian, Ruiqi Wang, Hongming Guo, Penghao Wu, Yuhao Dong, Xiuying Wang, Jingkang Yang, Hao Zhang, Hongyuan Zhu, and Ziwei Liu. Ego-r1: Chain-of-tool-thought for ultra-long egocentric video reasoning. *arXiv preprint*, 2025. 2
- [39] Ethan Waisberg, Joshua Ong, Mouayad Masalkhi, Nasif Zaman, Prithul Sarker, Andrew G Lee, and Alireza Tavakkoli. Meta smart glasses—large language models and the future for assistive glasses for individuals with vision impairments. *Eye*, 2024. 1, 4
- [40] Yanming Wan, Jiayuan Mao, and Josh Tenenbaum. Handmethat: Human-robot communication in physical and social environments. In *NeurIPS*, 2022. 1
- [41] Han Wang, Yanjie Wang, Yongjie Ye, Yuxiang Nie, and Can Huang. Elysium: Exploring object-level perception in videos via mllm. In *ECCV*, 2024. 2
- [42] Haochen Wang, Qirui Chen, Cilin Yan, Jiayin Cai, Xiaolong Jiang, Yao Hu, Weidi Xie, and Stratis Gavves. Object-centric video question answering with visual grounding and referring. In *ICCV*, 2025. 2
- [43] Xin Wang et al. Holoassist: an egocentric human interaction dataset for interactive ai assistants in the real world. In *ICCV*, 2023. 1
- [44] Junda Wu, Zhehao Zhang, Yu Xia, Xintong Li, Zhaoyang Xia, Aaron Chang, Tong Yu, Sungchul Kim, Ryan A. Rossi, Ruiyi Zhang, Subrata Mitra, Dimitris N. Metaxas, Lina Yao, Jingbo Shang, and Julian McAuley. Visual prompting in multimodal large language models: A survey. *arXiv preprint*, 2024. 2
- [45] Kun Yan, Lei Ji, Zeyu Wang, Yuntao Wang, Nan Duan, and Shuai Ma. Voila-a: Aligning vision-language models with user’s gaze attention. In *NeurIPS*, 2024. 1, 3
- [46] Jianwei Yang, Hao Zhang, Feng Li, Xueyan Zou, Chunyuan Li, and Jianfeng Gao. Set-of-mark prompting unleashes extraordinary visual grounding in gpt-4v. *arXiv preprint*, 2023. 2
- [47] Jingkang Yang et al. Egolife: Towards egocentric life assistant. In *CVPR*, 2025. 2, 6, 7
- [48] Haoxuan You, Haotian Zhang, Zhe Gan, Xianzhi Du, Bowen Zhang, Zirui Wang, Liangliang Cao, Shih-Fu Chang, and Yinfei Yang. Ferret: Refer and ground anything anywhere at any granularity. *arXiv preprint*, 2023. 2
- [49] Yuqian Yuan, Wentong Li, Jian Liu, Dongqi Tang, Xinjie Luo, Chi Qin, Lei Zhang, and Jianke Zhu. Osprey: Pixel understanding with visual instruction tuning. In *CVPR*, 2024. 2
- [50] Yuqian Yuan, Hang Zhang, Wentong Li, Zesen Cheng, Boqiang Zhang, Long Li, Xin Li, Deli Zhao, Wenqiao Zhang, Yueting Zhuang, Jianke Zhu, and Lidong Bing. Videorefer suite: Advancing spatial-temporal object understanding with video llm. In *CVPR*, 2025. 2
- [51] Duo Zheng, Shijia Huang, Yanyang Li, and Liwei Wang. Learning from videos for 3d world: Enhancing mllms with 3d vision geometry priors. In *NeurIPS*, 2025. 6, 7
- [52] Sheng Zhou, Junbin Xiao, Qingyun Li, Yicong Li, Xun Yang, Dan Guo, Meng Wang, Tat-Seng Chua, and Angela Yao. Egotextvqa: Towards egocentric scene-text aware video question answering. In *CVPR*, 2025. 2
- [53] Jinguo Zhu et al. Internvl3: Exploring advanced training and test-time recipes for open-source multimodal models. *arXiv preprint*, 2025. 4, 5, 6, 7

Do You See What I Am Pointing At?

Gesture-Based Egocentric Video Question Answering

Supplementary Material

Backbone	r	a	lr	Resolution
InternVL3-8B	64	128	1e-5	448×448
InternVL3-14B	32	64	2e-5	448×448
LLaVA-OneVision-7B	32	64	1e-5	384×384

Table 7. **Hyperparameters for HINT per backbone.** This table summarizes the optimized training configurations. Here, ‘r’ denotes the LoRA rank, ‘a’ the LoRA scaling factor, and ‘lr’ the learning rate used during finetuning.

A. Implementation Details

A.1. HINT Training Details

Table 7 summarizes the optimized hyperparameters used to finetune HINT on each backbone. We initialized the hyperparameter search around values commonly used in prior works and performed a grid search over LoRA rank and scaling factor pairs of $\{(8, 16), (16, 32), (32, 64), (64, 128)\}$ and learning rates in $\{2e-7, 1e-5, 2e-5\}$. The reported configurations were selected based on the best validation performance for each backbone.

In all experiments, we finetune only the LoRA adapters and the keypoint adapter while freezing the remaining backbone parameters. We use AdamW as the optimizer with a cosine learning rate schedule and a linear warm-up ratio of 0.03. Input videos are uniformly sampled in time to a fixed number of 32 frames, resized to the resolution in Tab. 7, and normalized following each backbone’s default preprocessing.

A.2. Evaluation Protocol

We evaluate all models using multiple-choice accuracy. Each example consists of a question, candidate options, and the index of the correct option. Models are instructed to answer by selecting an option letter (“A”, “B”, etc.). We handle several common output formats. If the entire string (after trimming whitespace) is a single option letter, we take it as the prediction. Otherwise, we progressively clean the output by stripping special markup such as `<answer>...</answer>`, as well as trailing control tokens (e.g., `<|im_end|>`) and boilerplate phrases (e.g., “Here’s the answer:”). After this cleaning step, we apply a sequence of regular expressions that search for: (i) a letter enclosed in parentheses, e.g., “(A)”; (ii) a letter followed by punctuation, e.g., “A.”, “B)” or “C]”; and (iii) an “Answer:” pattern at the end of the string, e.g., “Answer: D”. In all cases, we restrict matches to letters between “A” and the last valid option letter for that specific example. If a match

Method	Video-MME	MVBench	EgoSchema	EgoBlind
InternVL3-8B	64.2	73.2	67.2	52.8
HINT _{InternVL3-8B}	64.6	73.2	67.1	57.5

Table 8. **Performance on existing video understanding benchmarks.** Comparison of HINT against the baseline InternVL3-8B on Video-MME [15], MVBench [26], EgoSchema [28] (MCQ), and EgoBlind [11]. The results indicate that finetuning on our dataset preserves the model’s general video understanding capabilities.

is found and the letter is valid, we treat it as the model’s prediction and otherwise, we mark the prediction as invalid. Multiple-choice accuracy is computed as the fraction of examples for which the extracted option letter exactly matches the ground-truth option. For all baselines and HINT variants reported in the paper, we successfully extracted a valid option letter for every prediction, so the reported accuracies correspond to exact letter-wise matches without any manual corrections or post-hoc filtering.

B. Additional Analysis

B.1. HINT Performance on Existing Benchmarks

In Table 8, we report the performance of HINT on standard video understanding benchmarks to investigate whether finetuning on our proposed dataset compromises the model’s pretrained general capabilities. We compare our method with the backbone model, InternVL3-8B, on Video-MME [15], MVBench [26], and EgoSchema [28]. All evaluations use 32 uniformly sampled frames without any additional fine-tuning on the target benchmarks. This result demonstrates that the gesture-aware representations learned by HINT transfer positively to related egocentric assistive QA scenarios, even when explicit pointing gestures are absent in the target benchmark. As can be easily observed, HINT achieves comparable performance compared to the baseline. This demonstrates that our finetuning strategy effectively injects pointing gesture understanding capability without leading to catastrophic forgetting in general video understanding tasks, and also can be transfer positively to related egocentric assistive QA scenarios even when explicit pointing gestures are absent in the target benchmark.

B.2. Human Performance

We report the average accuracy of 5 participants. Each participant evaluated the full test set. The near-ceiling performance (total average 95.9%) confirms the questions are clear and easy for humans, yet reveals a substantial gap to

	Ref.	Temp.	Spat.	Count	Attr.	Feed.
Human	98.2	94.3	93.3	92.8	96.5	100.0

Table 9. **Human performance on EGOPOINTVQA.** We report the average accuracy of 5 human participants, each evaluating the full test set (672 questions).

Video	Reference	Temporal	Spatial	Attribute
Original	75.0	66.1	64.9	61.0
w/o Hand	41.7	21.4	44.4	36.3

Table 10. **Ablation study on the effect of hand gestures.** Performance comparison on our dataset with and without the pointing hand visible in the video frames. The significant drop in performance across all tasks in the ‘w/o Hand’ setting confirms that the pointing gesture is essential for identifying the target.

	Reference	Temporal	Spatial	Count	Attribute	Feedback
Random	20.0	20.0	27.0	20.0	20.0	50.0
Blind	16.7	25.5	32.0	6.3	22.5	54.9
Choices-only	20.8	25.5	20.8	10.4	21.6	54.1

Table 11. **Dataset bias analysis.** We evaluate two text-only baselines to detect potential shortcuts: ‘Blind’ receives the question text without video, and ‘Choices-only’ receives only the answer options without the question or video. Performance near random chance confirms that EGOPOINTVQA requires visual grounding. current MLLMs (best performing model 68.1%).

B.3. Effect of Hand Gestures in Video

To assess the importance of explicit pointing cues, we construct a static-video variant of EGOPOINTVQA in which the camera wearer’s hand is removed while keeping the rest of the scene and camera motion unchanged. We then evaluate models, including HINT, on this modified data using the same training and evaluation protocol as in the main experiments. Table 10 shows that removing hand gestures causes a large degradation in performance. This confirms that egocentric pointing cues are critical for resolving deictic references in EGOPOINTVQA.

B.4. Dataset Bias Analysis

To verify that EGOPOINTVQA does not contain unintended textual shortcuts, we evaluate two degenerate baselines that receive no visual input (Table 11). The **Blind** baseline feeds only the question text (without the video) to the model, testing whether the question wording alone leaks the answer. The **Choices-only** baseline provides only the multiple-choice options (without either the question or video), testing whether the answer can be guessed from the option distribution. Both baselines perform near random chance across all six task categories: Blind achieves 16.7–54.9% and Choices-only achieves 10.4–54.1%, closely matching the random baseline of 20.0–50.0%. These results confirm that EGOPOINTVQA genuinely requires visual grounding of pointing gestures to resolve deictic references, and that our question-answer generation pipeline does not introduce



Figure 7. **Representative failure cases on EGOPOINTVQA.** (a)-(b): baseline MLLM failures due to saliency bias and temporal confusion, respectively. (c)-(d): remaining HINT failures caused by unreliable hand keypoints and rapid viewpoint drift.

systematic textual or statistical shortcuts.

B.5. Failure Analysis

In Figure 7, we visualize example failure modes to better understand the limitations of both existing MLLMs and our proposed HINT.

Existing MLLM failure modes. We identify two dominant error patterns in baseline models. (a) *Saliency/center bias*: in cluttered scenes, models tend to predict a visually prominent or centrally located object rather than the one actually being pointed at. For example, the model may focus on a nearby blue shirt instead of the actual referent. (b) *Temporal confusion*: when multiple objects are sequentially pointed at, baseline models frequently confuse the temporal order, e.g., predicting the second pointed object when the question asks about the first. HINT mitigates both failure modes by providing frame-aligned 3D hand geometry that explicitly anchors deictic references to the correct spatial and temporal locations.

Remaining HINT failure modes. Despite the overall improvements, HINT fails under certain challenging conditions. (c) *Unreliable gesture signal*: when the hand is affected by motion blur or partial occlusion, the 3D hand reconstruction from WiLoR becomes noisy. In such cases, the hand detection confidence may fall below the threshold τ , resulting in absent hand intent tokens, or the tokens may encode misleading pose information. (d) *Rapid viewpoint drift*: fast head movements can cause the target object to leave the camera’s field of view entirely, making it harder for the model to associate the gesture with the correct referent regardless of the quality of hand tokens. These remaining errors are largely attributable to input signal quality rather than architectural limitations, suggesting that advances in robust hand pose estimation and temporal object tracking under egocentric motion would yield further gains.

C. EGOPOINTVQA

In this section, we provide additional analysis of EGOPOINTVQA, qualitative visualizations, and a detailed description of the question answer pair generation pipeline.

C.1. Video Collection Details

Participants. We recruit 20 participants from 12 nationalities (11 female, 9 male; ages 18–45) to collect the real-world portion of EGOPOINTVQA. The diverse participant pool ensures variation in hand shape, skin tone, and pointing style, which encourages models to generalize across different users rather than overfitting to a narrow demographic.

Scenes and activities. Real-world videos are captured across a broad variety of settings, including offices, kitchens, living rooms, streets, train platforms, and balconies. Activities during recording span desk work, organizing, artwork, and cooking, reflecting natural everyday scenarios in which pointing gestures commonly occur. Of the 400 collected videos, 360 are recorded in indoor environments and 40 in outdoor settings.

Capture protocol. Each participant wears Meta Ray-Ban smart glasses and is instructed to point with one hand using an extended index finger for at least 2 seconds at objects of their choice. We require that more than 3 objects are visible in the scene to ensure sufficient visual complexity for generating challenging deictic questions. Each clip ranges from 3–8 seconds at 30 FPS with a resolution of 1536×2048 .

Data Split	# Vid.	# QA	Vid. Dur.(s)	# Obj.
Train(Real)	100	640	4.61	22.5
Train(Synthetic)	4,000	18,745	11.6	11.6
Test (Real)	300	672	5.05	16.5

Table 12. **EGOPOINTVQA statistics.** Statistics of the dataset across synthetic and real-world splits. Real-world clips generally feature higher object density (scene complexity) than synthetic clips.

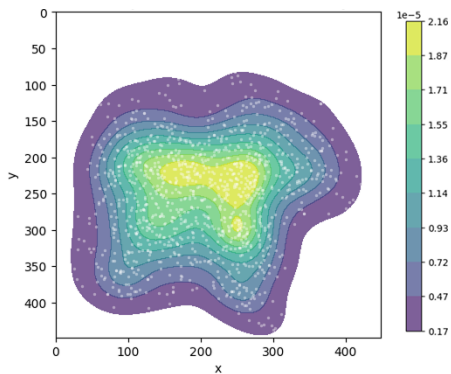


Figure 8. **Spatial distribution of target objects in EGOPOINTVQA.** ‘x’ and ‘y’ axes refer to the horizontal and vertical pixel coordinates, respectively. Individual object locations are shown as scattered dots.

C.2. Dataset Statistics

Table 12 summarizes the scale and complexity of EGOPOINTVQA. The dataset is composed of a large-scale synthetic training set (4,000 videos) to encourage robust generalization, complemented by real-world data for domain adaptation and testing. Notably, the real-world videos contain a higher density of objects (avg. 22.5 and 16.5 per video) compared to the synthetic set (avg. 11.6 per video), presenting a greater challenge in grounding target pointed objects.

In Fig. 8, we visualize the spatial distribution of target objects by their center coordinate within the frame. While there is a natural center bias typical of egocentric videos, where users tend to center objects they interact with, the heatmap demonstrates a diverse distribution of the object location. This broad distribution confirms that models cannot rely solely on center priors and must utilize the pointing gestures to resolve references.

C.3. Extended Visualization of EGOPOINTVQA

We provide additional qualitative examples from the real-world split of EGOPOINTVQA in Figures 19 and 20. Figure 19 presents samples recorded in **indoor environments**, illustrating various household objects and close-range pointing gestures. In contrast, Figure 20 depicts sequences captured in **outdoor settings**. These visualizations showcase the range of scenes and contexts included in the collected data.

C.4. Synthetic Video Generation

We generate synthetic egocentric videos using the AI2-THOR simulator [23] running in Unity. Our implementation utilizes AI2-THOR commit 0+8524ea and Unity version 2020.3.25f1. The video generation process follows four steps.

First, we randomly sample a scene, an agent location, and a head camera orientation. We keep only viewpoints where at least three objects are simultaneously visible according to ground-truth instance segmentation masks from the simulator.

From the visible entities, we select a target object of the pointing gesture. To ensure valid grounding, we require the object to meet two criteria: more than 10% of its pixels must be visible, and its depth must be within 2.0 meters from the agent.

For the target object, we retrieve a pointing animation from the MIXAMO [21] library that possesses the most similar initial pose to the required trajectory. We then apply Inverse Kinematics (IK) to refine the avatar’s arm and hand configuration, forcing the index finger to align precisely with the target object.

After IK adjustment, we verify that the pointing ray originating at the fingertip intersects the 3D bounding box of

the target. If the pointing deviates or misses the target, we discard this sample and resample a new viewpoint/pose.

C.5. Automatic Question and Answer Generation Details

We provide a detailed breakdown of the prompts and logic used in our three-stage generation pipeline described in the main paper (§ 3.3). We utilize InternVL3-78B [53] for scene information extraction and multiple-choice question-answer pair generation (Stages 1& 2) and GPT-4o [20] for linguistic refinement and quality control (Stage 3).

Stage 1: Dense scene information extraction. Instead of generic captions, we require structured scene graphs to ground the subsequent QA generation. As shown in Fig. 9, we prompt the annotator MLLM to act as a Dense Scene Fact Miner.” The model analyzes the video frames and outputs a JSON list of all salient objects. To ensure high-quality grounding, we enforce two strict constraints in the prompt: (1) Hand-Agnostic Descriptions: The model is explicitly forbidden from describing human interaction (e.g., pointed by a hand) to ensure object attributes are described objectively based on their visual state. (2) Discriminative Expressions: If multiple instances of the same category exist, the model must generate unique referring expressions to distinguish them.

Stage 2: Target-specific multiple-choice question answer generation. We generate the question stem and the multiple-choice options in two sequential sub-steps to ensure logical consistency.

Stage 2-1: Question-answer pair generation. First, we feed the scene JSON from Stage 1 and a list of target object IDs into the MLLM. We use a modular prompting approach: a general instruction template (Fig. 10) is combined with specific **Task Modules** depending on the question category. The General Template enforces that the answer must be derived *exclusively* from the provided scene JSON to prevent hallucinations. The Task Modules contain specific logic for our six tasks: Reference (Fig. 11), Attribute (Fig. 12), Spatial (Fig. 13), Feedback (Fig. 14), Counting (Fig. 15), and Temporal (Fig. 16).

Stage 2-2: Negative choices generation. To convert the QA pairs into challenging Multiple-Choice Questions (MCQs), we prompt the model to generate distractors based on the specific question type, as detailed in Fig. 17. For binary questions, the model is restricted to “Yes/No” options. For open-ended questions, we instruct the model to generate four “Hard Negatives” using a prioritized strategy: (1) Visible Sources: Attributes or locations of *neighboring* objects in the scene (e.g., if the target is red, select the color of a nearby blue cup). (2) Plausible Fakes: Attributes that are semantically valid for the category but visually incorrect. (3) Logical Opposites: For spatial or temporal relations (e.g., “Left” vs. “Right”).

Stage 3: Deictic question rephrasing. In the final stage, we prompt GPT-4o to transform the structured, robotic questions into natural, spoken egocentric queries (Fig. 18). The prompt acts as both a linguistic rephraser and a quality control. The model is instructed to replace target placeholders with deictic pronouns (“this”, “that”), while preserving the names of reference objects (anchors) that are not being pointed at (e.g., “Is **this** closer than the red book?”). Here, we enforce that the rephrased question must be ambiguous if read without seeing the pointing gesture.

Stage 1: Dense Scene Information Extraction

```
### Role:
You are a highly perceptive visual analysis expert, acting as a "Dense Scene Fact Miner."

### Task:
Analyze the provided video frames and generate a comprehensive, structured description of ALL salient objects visible in the scene.

### CONSTRAINT
1. Hand-Agnostic: You MUST NOT mention "hand," "fingers," "arm," or "person" in the object descriptions. -
BAD: "held by a hand," "being moved by a user."
- GOOD: "The object is moving upwards," "situated on the table."
2. Discrimination: If multiple objects of the same category are present (e.g., three different bottles), you MUST provide unique `referring_expressions` and `attributes` for each so they can be distinguished (e.g., "The green glass bottle" vs "The clear plastic bottle").

### OUTPUT FORMAT (Strict JSON List)
Return a single JSON list containing a dictionary for every significant object visible.
```json [ { "id": "object_01", "identity": "The common name (e.g., 'glass jar').", "object_category": "Broad category (e.g., 'container').", "part_level": "Description if it is a part (e.g., 'lid'), otherwise null.", "referring_expression": "A unique phrase distinguishing this object from others (e.g., 'the tall glass jar on the left').", "attributes": { "color": "Specific color.", "material": "Apparent material.", "shape": "Primary shape.", "contents": "Visible contents (e.g., 'pasta', 'empty').", "state": "Condition (e.g., 'open', 'closed', 'dirty').", "temporal_summary": "Concise summary of this specific object's movement or lack thereof (e.g., 'Stationary throughout').", "function": "Typical purpose (e.g., 'storing food').", "spatial_location": "Location relative to the scene (e.g., 'On the middle shelf, next to the red bowl')." }, { "id": "object_02", ... } ]
```

### Instruction:
1. Scan the scene from left to right, foreground to background.
2. Identify every distinct, salient object.
3. Generate the JSON list strictly following the structure above.
```

Figure 9. **Prompt used for dense scene information extraction (Stage 1).** Instructions given to the MLLM to extract a structured JSON list of all salient objects.

Stage 2-1: Target-Specific Question Answer Pair Generation Template

```
### Role:
You are an expert region-level question answer generator for egocentric video datasets.

### Goal:
Generate 5 diverse and logically challenging Question-Answer pairs based on the provided scene data.

### Inputs:
• [TARGET_IDS]: An ordered list of object IDs to focus on (e.g., ["<obj_1>", "<obj_5>"]).
• [OBJECTS_DATA]: The JSON list of all visible objects (containing attributes, locations, and functions).

### Instruction:
1. Generate a total of 5 questions. using the placeholder <obj_ID>.
2. Always refer to the target object using its ID (e.g., <obj_5>).
3. The `correct_answer` must be derived *exclusively* from the provided JSON data. Do not hallucinate properties.
4. Do not stick to simple "What is X?" questions. Use comparisons, negations, and scenario-based phrasing where possible.

### Output format:
Return a single JSON list containing 5 objects.
```json
[{ "target_id": "<obj_X>", "question": "The generated question string with placeholders", "answer": "The exact ground truth string", ... (total of 5) }]
```

<<TASK-SPECIFIC PROMPT & Examples>>

### TARGET_IDS: <<taret_object_ids>>
### OBJECTS_DATA: <<stage1_output>>
```

Figure 10. **General template for QA pair generation (Stage 2-1).** The base instruction template is used for all question types. It enforces that the "correct answer" must be derived exclusively from the scene JSON provided in Stage 1 to prevent hallucinations.

Stage 2-1: Target-Specific Question Answer Pair Generation - Reference

```
### TASK DESCRIPTION: REFERENCE
**Goal:** Test the model's ability to identify the object's category or specific identity.
**Rules:**
1. **Identity:** Ask for the name/category (e.g., "What is <obj_X>?").
2. **Differentiation:** If there are similar objects (e.g., two cups), ask a question that confirms specific identity (e.g., "Is <obj_X> the red cup or the blue cup?").
3. **Negation:** Ask what the object is *not* (e.g., "Is <obj_X> a laptop?").

### EXAMPLE
**Input:**
TARGET_IDS:
[<obj_1>, <obj_2>]
OBJECTS_DATA:
[{"obj_id": "<obj_1>", "identity": "Espresso Machine", "object_category": "Appliance"},
{"obj_id": "<obj_2>": "Coffee Grinder", "object_category": "Appliance"}, ...]

**Output:**
[
  {
    "target_id": "<obj_1>",
    "question": "What specific appliance is <obj_1>?",
    "answer": "Espresso Machine"
  },
  {
    "target_id": "<obj_2>",
    "question": "What is <obj_2>?",
    "answer": "Coffee Grinder"
  }
]
```

Figure 11. **Task-specific prompt for Reference QA generation.** This task directs the model to generate questions that require identifying the specific description or category of the pointed-at object (e.g., "What is this?").

Stage 2-1: Target-Specific Question Answer Pair Generation - Attribute

```
### TASK DESCRIPTION: ATTRIBUTE
**Goal:** Test the model's perception of fine-grained visual details.
**Rules:**
1. **Direct Query:** Ask for a specific attribute value from the JSON (Color, Shape, Material, State).
2. **Comparison:** Compare the target to another visible object (e.g., "Is <obj_X> the same material as <obj_Y>?").
3. **State:** Ask about the condition (e.g., "Is <obj_X> currently open or closed?").

### EXAMPLE
**Input:**
TARGET_IDS:
["<obj_1>", "<obj_2>"]
OBJECTS_DATA:
[
  {"obj_id": "<obj_1>", "identity": "Red Apple", "attributes": {"color": "red", "state": "whole"}},
  {"obj_id": "<obj_2>", "identity": "Green Apple", "attributes": {"color": "green", "state": "sliced"}}
]

**Output Generation:**
[
  {
    "target_id": "<obj_1>",
    "question": "What is the color of <obj_1>?",
    "answer": "Red"
  },
  {
    "target_id": "<obj_1>",
    "question": "Is <obj_1> sliced like <obj_2>?",
    "answer": "No"
  }
]
```

Figure 12. **Task-specific prompt for Attribute QA generation.** This module focuses on fine-grained visual details, instructing the model to query properties such as color, shape, material, or state (e.g., "Is this sliced?").

Stage 2-1: Target-Specific Question Answer Pair Generation - Spatial

```
### TASK DESCRIPTION: SPATIAL
**Goal:** Test the model's understanding of relative position and depth.
**Rules:**
1. **Relative Location:** Ask where the target is relative to a landmark object (e.g., left/right/above/below).
2. **Proximity:** Ask about distance (e.g., "Is <obj_X> closer to the sink than <obj_Y>?").
3. **Constraint:** You MUST verify the relationship using the provided `spatial_location` or scene description in the JSON.

### EXAMPLE
**Input:**
TARGET_IDS:
["<obj_1>", "<obj_2>"]
OBJECTS_DATA:
[
  {"obj_id": "<obj_1>", "identity": "Sponge", "spatial_location": "Inside the sink", "bbox": [x1,y1,x2,y2]},
  {"obj_id": "<obj_2>", "identity": "Soap dispenser", "spatial_location": "To the right of the sink", "bbox": [x1,y1,x2,y2]},
  {"obj_id": "<obj_3>", "identity": "Sink", "spatial_location": "Next to the fridge", "bbox": [x1,y1,x2,y2]}
]

**Output Generation:**
[
  {
    "target_id": "<obj_1>",
    "question": "Where is <obj_1> located relative to the sink?",
    "answer": "Inside"
  },
  {
    "target_id": "<obj_2>",
    "question": "Is <obj_2> to the left of the sink?",
    "answer": "No"
  }
]
```

Figure 13. **Task-specific prompt for Spatial QA generation.** This task generates questions regarding the relative position or depth of the target object compared to other landmarks in the scene (e.g., “Is this to the left of the sink?”).

Stage 2-1: Target-Specific Question Answer Pair Generation - Feedback

```
### TASK DESCRIPTION: FEEDBACK
**Goal:** Test reasoning about user intent, affordance, and safety.
**Rules:**
1. **Goal Suitability:** Create a user goal (e.g., "I am thirsty") and ask if the target is suitable.
2. **Comparison:** Ask which object is better for a specific task.
3. **Safety:** Ask if an interaction is safe based on attributes (e.g., "Can I put <obj_X> (metal) in the microwave?").

### EXAMPLE
**Input:**
TARGET_IDS:
["<obj_1>", "<obj_2>"]
OBJECTS_DATA:
[
  {"obj_id": "<obj_1>", "identity": "Glass Vase", "function": "Decoration", "attributes": {"material": "Glass"}},
  {"obj_id": "<obj_2>", "identity": "Plastic Cup", "function": "Drinking", "attributes": {"material": "Plastic"}}
]

**Output Generation:**
[
  {
    "target_id": "<obj_2>",
    "question": "I am thirsty. Should I use <obj_2> to drink water?",
    "answer": "Yes"
  },
  {
    "target_id": "<obj_1>",
    "question": "Is <obj_1> suitable for drinking water?",
    "answer": "No"
  }
]
```

Figure 14. **Task-specific prompt for Feedback QA generation.** This task tests reasoning about user intent and affordance, generating questions about whether a specific object is suitable for a stated goal (e.g., “I am thirsty. Can I drink this?”).

Stage 2-1: Target-Specific Question Answer Pair Generation - Counting

```
### TASK DESCRIPTION: COUNTING
**Goal:** Test visual search and enumeration of number of objects.
**Rules:**
1. Identify the category of the target (e.g., "Bottle"). Count ALL objects in `OBJECTS_DATA` that share this category.
2. Ask "How many of these (<obj_X>) are there?"
3. Ensure the question specifies what to count (e.g., "How many red objects...", "How many bottles...").

### EXAMPLE
**Input:**
TARGET_IDS:
["<obj_1>", "<obj_3>"]
OBJECTS_DATA:
[
  {"obj_id": "<obj_1>", "object_category": "Pen", "attributes": {"color": "Blue"}},
  {"obj_id": "<obj_2>", "object_category": "Pen", "attributes": {"color": "Red"}},
  {"obj_id": "<obj_3>", "object_category": "Pencil", "attributes": {"color": "Yellow"}}
]

**Output Generation:**
[
  {
    "target_id": "<obj_1>",
    "question": "How many of <obj_1> are visible in the scene?",
    "answer": "2"
  },
  {
    "target_id": "<obj_3>",
    "question": "How many of <obj_3> are there?",
    "answer": "1"
  }
]
```

Figure 15. **Task-specific prompt for Counting QA generation.** This task tests visual search capabilities by asking the model to enumerate instances of the pointed-at object category visible in the scene.

Stage 2-1: Target-Specific Question Answer Pair Generation - Temporal

```
### TASK DESCRIPTION: TEMPORAL
**Goal:** Test the model's ability to recall the chronological sequence of interactions.
**Critical Assumption (The Timeline):** The `TARGET_IDS` list provided in the input acts as the Interaction Log.
* Index 0 = The 1st object pointed at.
* Index 1 = The 2nd object pointed at.
* Index N = The (N+1)th object pointed at.
* Note: Ignore the numeric digits in the ID itself (e.g., `<obj_2>` might appear before `<obj_1>`).

**Rules:**
1. Ordinality: Ask "What is the [First/Second/Last] object pointed at?"
2. Relative Sequence: Ask "Did I point to <obj_X> before/after <obj_Y>?"
3. Attribute Recall: "What was the color of the object I pointed at before <obj_X>?"

### EXAMPLE
**Input:**
TARGET_IDS:
["<obj_2>", "<obj_1>"]
*(Meaning: First interaction was <obj_2>, Second interaction was <obj_1>)*

OBJECTS_DATA:
[
  {"obj_id": "<obj_1>", "identity": "Lamp", "attributes": {"color": "Silver"}},
  {"obj_id": "<obj_2>", "identity": "Book", "attributes": {"color": "Red"}}
]

**Output Generation:**
[
  {
    "target_id": "<obj_1>",
    "question": "What is the second object I pointed at?",
    "answer": "Lamp"
  },
  {
    "target_id": ["<obj_1>", "<obj_2>"],
    "question": "Did I point at <obj_1> after <obj_2>?",
    "answer": "Yes"
  }
]
```

Figure 16. **Task-specific prompt for Temporal QA generation.** This task challenges the model's ability to recall the chronological sequence of pointing gestures (e.g., "What is the second object I pointed at?").

Stage 2-2: Negative Choices Generation

```
### Role:
You are an expert Multiple-Choice Question Generator specializing in "Hard Negative" mining.

### Task:
Analyze a pre-generated Question-Answer pair and generate high-quality distractors to complete the Multiple Choice Question (MCQ).

### DISTRACTOR RULES
1. Case 1: Binary Questions (Yes/No)
* **Trigger:** If question starts with "Is", "Are", "Do", "Does", "Did", "Can", "Should".
* **Action:** Generate **only two options**: "(A) yes", "(B) no".

2. Case 2: Standard Questions (Open-ended)
• Trigger: All other questions (What, Where, How many, Which).
• Action: Generate **4 distractors** (Total 5 options including the answer).
• Strategy:
  1. **[Visible Source]** (Highest Priority) Pick attributes/locations of **other visible objects** in `SCENE_CONTEXT`.
  2. **[Plausible Fake]** Invent values that make sense for the category but are wrong.
  3. **[Logical Opposite]** For spatial (e.g., Left vs Right).

### OUTPUT FORMAT
Return the exact input JSON, but append `options` and `distractor_rationale`.

### EXAMPLE (Standard)
**Input:** {"question": "What material is <obj_1>", "answer": "Glass", "target_id": "<obj_1>"}OBJECTS_DATA
**Output:**
```json
{
 "target_id": "<obj_1>",
 "question": "What material is <obj_1>",
 "answer": "Glass",
 "options": ["(A) Wood", "(B) Plastic", "(C) Glass", "(D) Metal", "(E) Ceramic", "(F) Paper"],
 "distractor_rationale": {
 "Wood": "Source: Visible Source (Table). Rationale: Confusing target with nearby object."
 }
}
```

Figure 17. Prompt used for negative choices generation (Stage 2-2). Instructions for generating negative choices. The model is prompted to select attributes from neighboring objects or plausible but incorrect properties to create challenging multiple-choice options.

## Stage 3: Deictic Question Rephrasing

```
Role: You are a linguistic expert and Quality Control Auditor for an Egocentric Video dataset.

• Input:
A JSON list of structured question objects (containing question, options, answer, and metadata).

Task:
Transform the robotic question string (e.g., "What is <obj_1>") into a natural, spoken question using deictic pronouns ("this", "that").

Criteria:
You must evaluate every rephrased question against these two rules. If a question cannot satisfy both, DISCARD IT (do not include it in the output).
i. Deictic Ambiguity (The "Blindfold" Test): The rephrased question MUST BE AMBIGUOUS if read without seeing the video.
• CONSTRAINT: You MUST NOT reveal the identity of the target object in the question stem.
• Bad (Too specific): "What color is this apple?" (FAIL: The user knows it's an apple without looking).
• Bad (Too specific): "Is the mug to the left of the jar?" (FAIL: The user knows the target is a mug).
• Good (Ambiguous): "What color is this?" (PASS: User must look at the pointing gesture).
• Good (Ambiguous): "Is this to the left of the jar?" (PASS).
ii. Correctness & Preservation: The rephrased question must strictly maintain the original logic so the answer remains correct.
• CONSTRAINT: Do not change the question type. If the original asked for "Material", do not change it to "Texture".
• CONSTRAINT: Do not alter the options or answer fields.

REPHRASING INSTRUCTIONS
i. Target Replacement: Replace the target object ID (e.g., <obj_1>) with "this", "that", "it", "these", or "the one".
ii. Reference Preservation: If the question compares the target to a second object (that is NOT being pointed at), refer to the second object by its natural name (e.g., "the red book") to ensure the sentence is grammatically coherent.
• Example: "Is <obj_1> closer than <obj_2>?" -> "Is this closer than the red book?"

OUTPUT FORMAT
Return a JSON list of the valid, filtered objects.
If a question fails the criteria and cannot be fixed, exclude it from the list.
Now, rephrase the provided question answer pair.

INPUT:
<<stage_2_output_json>>

OUTPUT:
```

Figure 18. Prompt used for deictic question rephrasing (Stage 3). The final prompt in the pipeline, where GPT-4o acts as a linguistic expert to convert structured queries into natural, spoken questions. It replaces explicit object names with deictic pronouns ("this", "that") to ensure the question requires visual grounding to be answered.



Question: What is the first object I pointed at?  
Options: (A) Cellphone (B) Charger (C) Hard drive (D) Headphones (E) Apple

Temporal



Question: How many of these items are visible?  
Options: (A) 2 (B) 3 (C) 4 (D) 5 (E) 6

Counting



Question: What is the color of this?  
Options: (A) Yellow (B) Pink (C) Purple (D) Orange (E) Red

Attribute



Question: Is this on the left of the fork?  
Options: (A) yes (B) no

Spatial



Question: I want to serve some soup. Which object is more appropriate to use, first indicated object or second pointed object?  
Options: (A) first indicated object (B) second pointed object

Feedback

Figure 19. Examples from real-world indoor scenes. Samples from the real-world split of the dataset, captured in indoor environments. Each row displays the sample video frames alongside the corresponding question-answer pair generated by our pipeline. The correct answer is bolded and underlined within the options.



Question: Is the second pointed one further from me than the first one?  
Options: (A) yes (B) no

Spatial



Question: How many instances of the object I am pointing are there?  
Options: (A) 1 (B) 2 (C) 3 (D) 4 (E) 5

Counting



Question: What is that?  
Options: (A) A building (B) A tree (C) A river (D) A boat (E) A dock

Reference



Question: What is that on the pole used for?  
Options: (A) power pole (B) CCTV (C) light (D) decoration (E) speaker

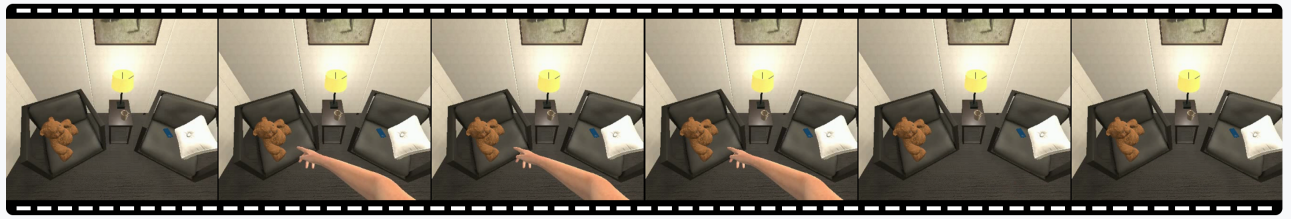
Feedback



Question: In which order is this door from the left?  
Options: (A) first (B) second (C) third (D) fourth (E) fifth

Spatial

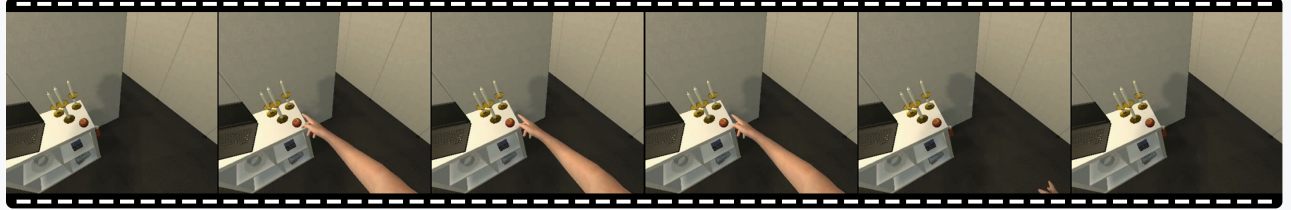
Figure 20. **Examples from real-world outdoor scenes.** Samples from the real-world split of the dataset, captured in outdoor environments. Each row displays the sample video frames alongside the corresponding question-answer pair generated by our pipeline. The correct answer is bolded and underlined within the options.



Question: What is this?

Options: (A) A desk lamp (B) A pillow (C) A painting (D) **A teddy bear** (E) A cup

Reference



Question: How many instances of this are visible?

Options: (A) 1 (B) 2 (C) **3** (D) 4 (E) 5

Counting



Question: Is it farther from me than the book?

Options: (A) Yes (B) **No**

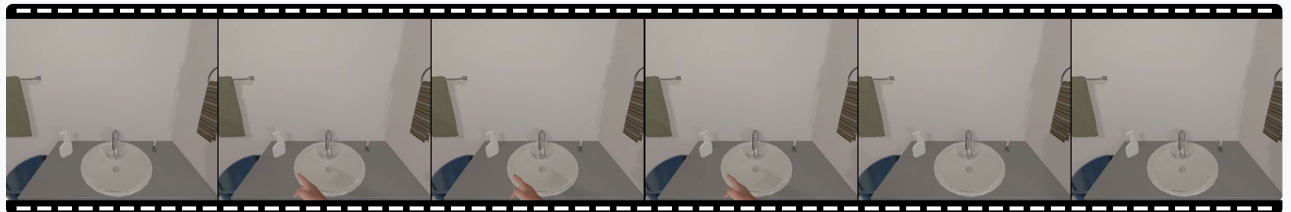
Spatial



Question: What is the second object I pointed at?

Options: (A) A chair (B) A book (C) A bed (D) **A hand-shaped statue** (E) A dog-shaped statue

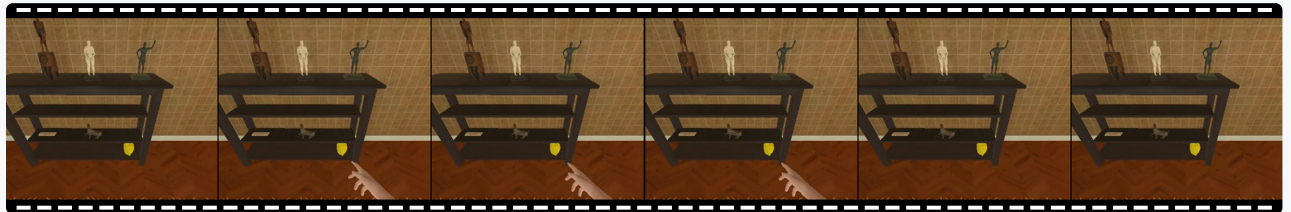
Temporal



Question: I want to dry my hands. Should I use this one?

Options: (A) yes (B) **no**

Feedback



Question: What is the main color of that?

Options: (A) White (B) Brown (C) **Yellow** (D) Green (E) Grey

Attribute

Figure 21. **Examples from synthetic training data.** Samples from the large-scale synthetic training set generated via AI2-THOR.